

ACCEPTED PAPER · SUPPLEMENTARY FILE

## Engineering a biocompatible 3D model of the bone marrow niche for drug screening against KMT2A-rearranged acute myeloid leukaemia cell line MOLM-13

*Paper version: Accepted Paper*

Accepted Papers are manuscripts accepted for publication, encompassing all changes made following the peer review process, along with a standard cover page indicating the paper version and an “Accepted Paper” watermark, but excluding any other editing, typesetting or other changes made by AccScience Publishing and/or authors post-acceptance.

**Article ID:** IJB026190172

**Citation:** Hope L, Sanchez-Rubio A, Berry C, Salmeron-Sanchez M, Copland M, Wheadon H. Engineering a biocompatible 3D model of the bone marrow niche for drug screening against KMT2A-rearranged acute myeloid leukaemia cell line MOLM-13. *Int J Bioprint*. 2026. doi: 10.36922/IJB026190172

**Copyright:** © 2026 Author(s). This is an Open Access article distributed under the terms of the Creative Commons Attribution License, permitting distribution, and reproduction in any medium, provided the original work is properly cited.

**Publisher’s Note:** AccScience Publishing remains neutral with regard to jurisdictional claims in published maps and institutional affiliations.

**Engineering a biocompatible 3D model of the bone marrow niche for drug screening against *KMT2A*-rearranged acute myeloid leukaemia cell line MOLM-13**

*Running title:* Bioprinted leukaemia model for drug screening

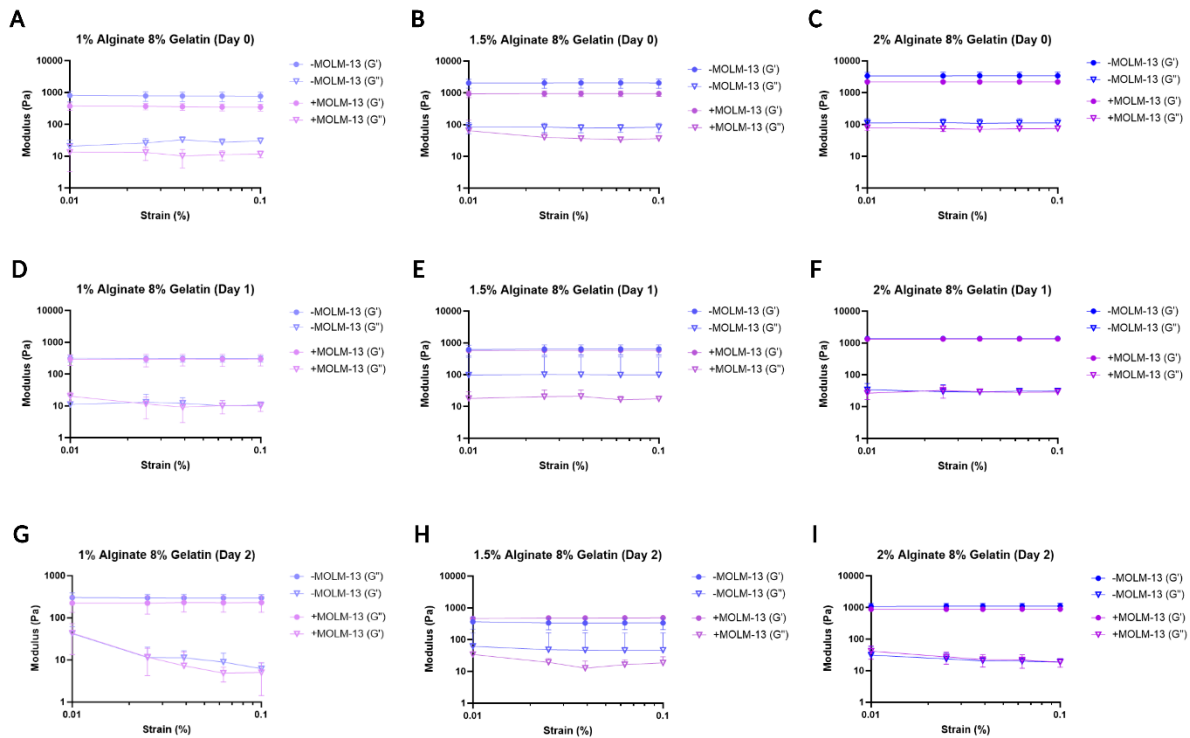
**Supplementary File**

**(A) Supplementary methods**

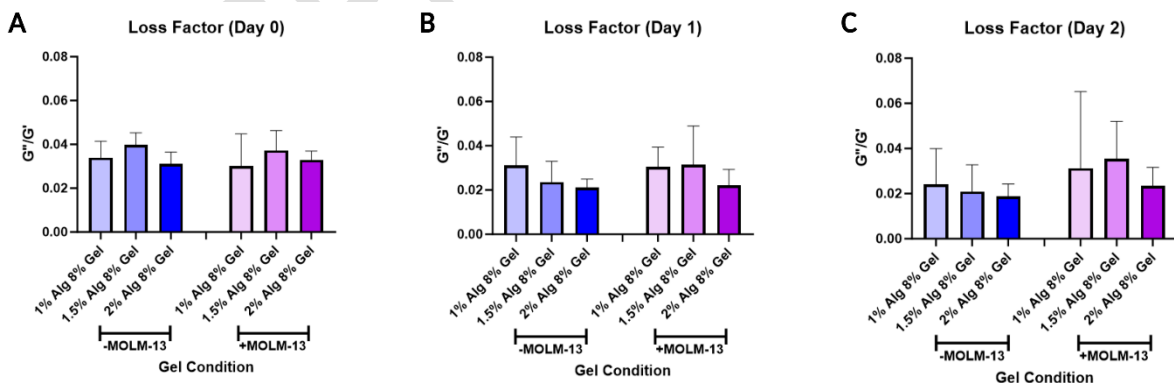
*Actin/DAPI staining*

2%Alg 8%Gel hand-cast and 3D bioprinted hydrogels containing MOLM-13 cells or MOLM-13 HS5 spheroid co-culture were washed in PBS supplemented with calcium and magnesium (PBS+; Gibco), then fixed in 4% paraformaldehyde in PBS+ at 37 °C for 15 minutes. Hydrogels were washed with PBS+ then permeabilised (10.3 g sucrose, 0.292 g sodium chloride, 0.06 g magnesium chloride (hexahydrate), 0.476 g HEPES in 100 mL PBS+, 0.5 mL Triton X) for five minutes at 4°C. Gels were washed with PBS+ then blocked in 1% bovine serum albumin (BSA) for five minutes at 37°C. Gels were submerged in 1% BSA containing Alexa Fluor™ 594 Phalloidin stain (Invitrogen) and incubated for 1 hour at 37°C. After incubating, the gels were washed three times with 0.5% PBS+-Tween20 under gentle agitation. Gels were stained with VECTASHIELD Antifade mounting media containing DAPI (Vector Laboratories, USA) prior to imaging. Images were captured at 10X and 20X magnification using the Zeiss Axiovert (hand-cast) and EVOS M7000 Imager (3D bioprinted) (Ex/Em: Alexa Fluor™ 594 Phalloidin: 581/609 nm; DAPI: 360/460 nm).

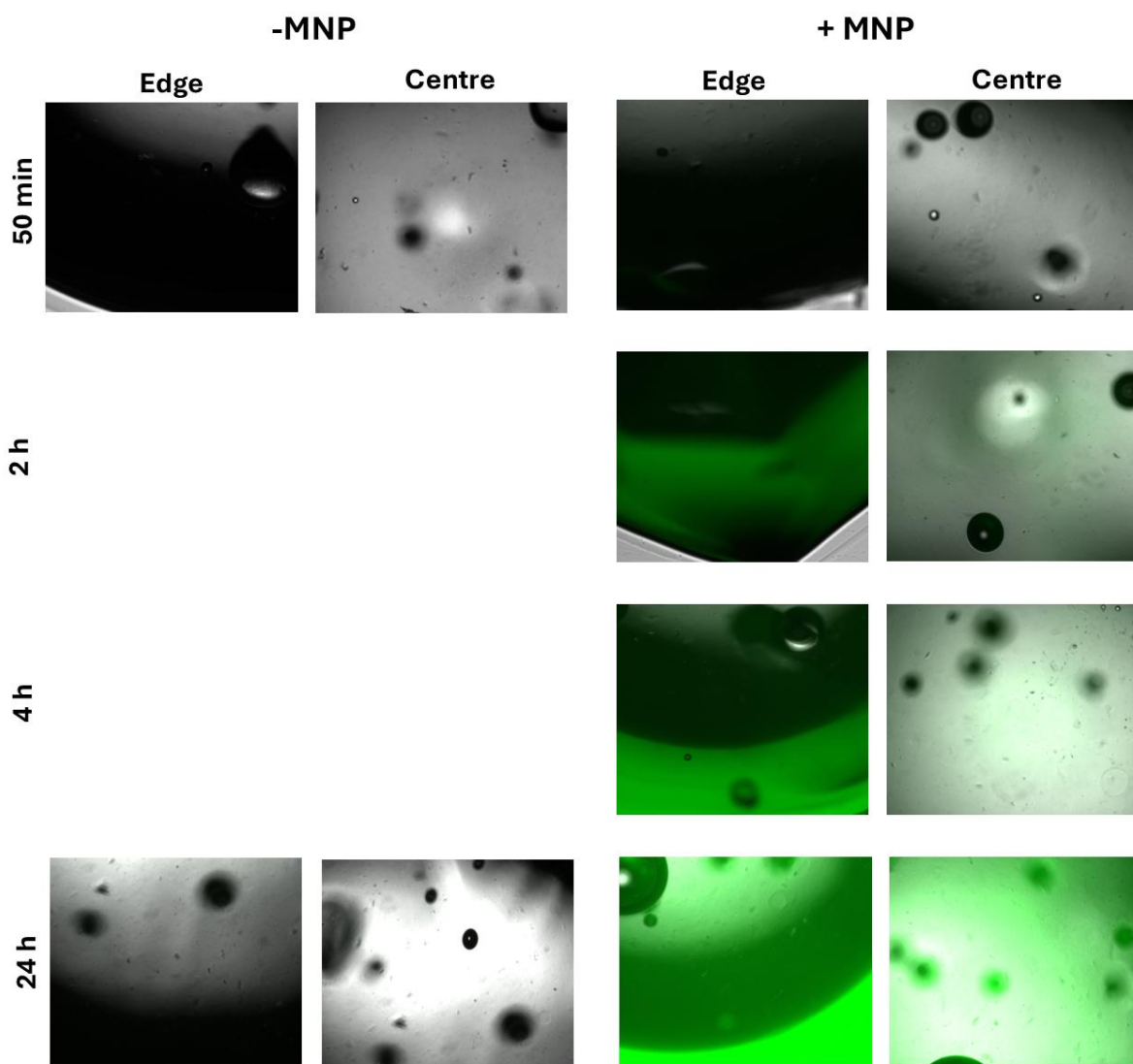
## (B) Supplementary figures and tables



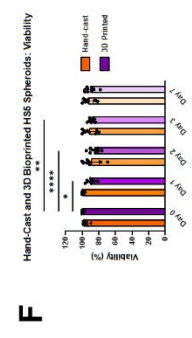
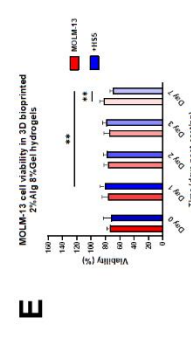
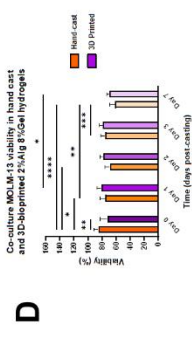
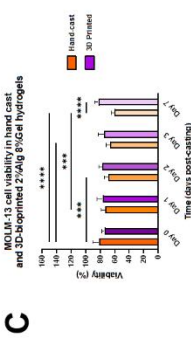
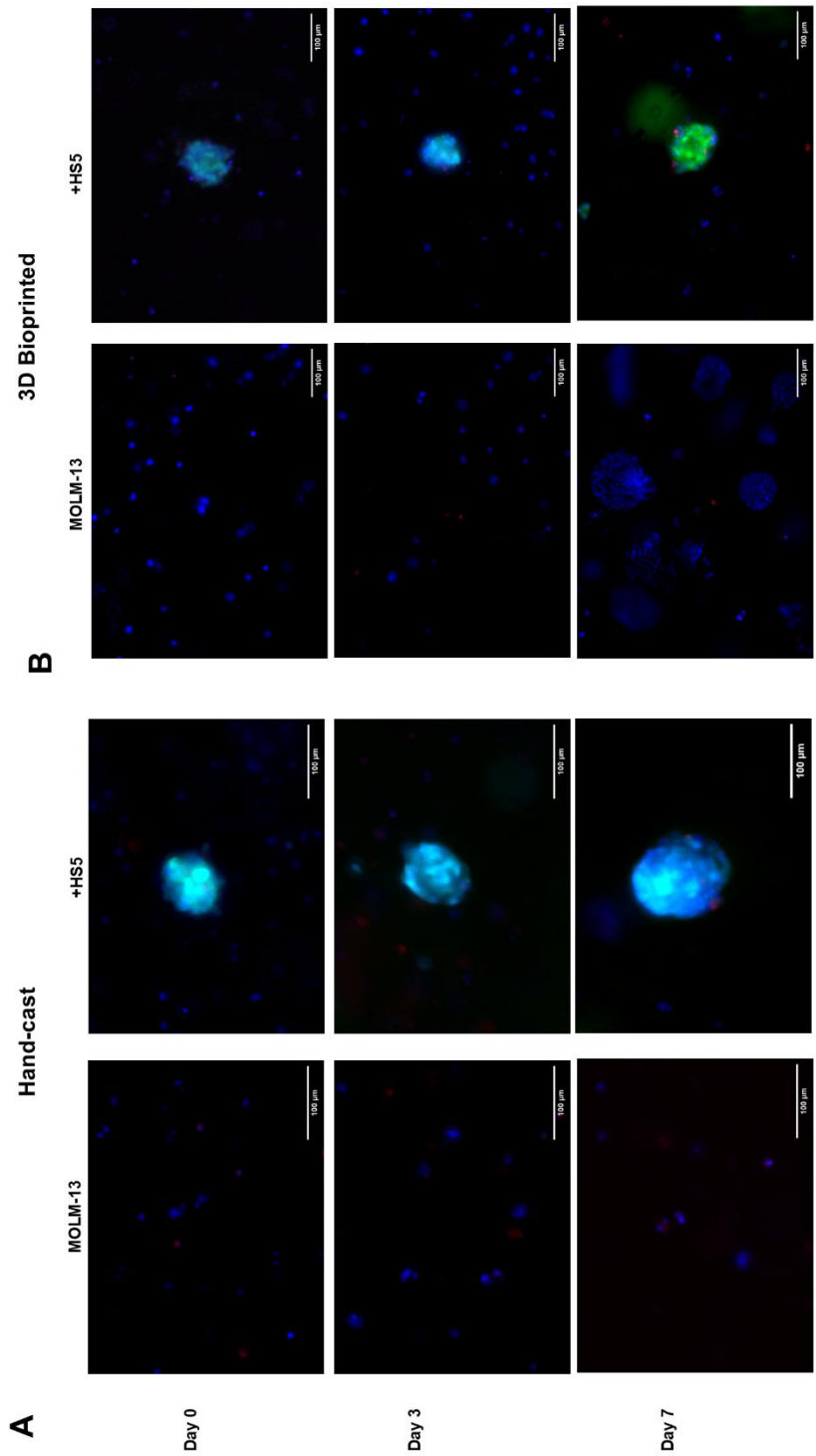
**Supplementary Figure 1: Strain sweeps of 1%, 1.5% and 2% Alg 8% Gel hydrogels at days 0, 1 and 2 after crosslinking.** A, D and E depict 1%Alg 8%Gel at days 0, 1, 2 respectively; B, E and H depict 1.5% Alg 8%Gel hydrogels; and C, F, I show 2%Alg 8%Gel. Closed circles show the storage modulus ( $G'$ ) and open triangles show the loss modulus ( $G''$ ). Strain range was 0.01-0.1% strain and angular frequency was 10 rad/s. Error bars depict standard deviation.



**Supplementary Figure 2: Loss factor of 1%, 1.5% and 2% Alginate/8% gelatin hydrogels with and without MOLM-13 cells over two days.** Loss factor was calculated as outlined in equation 2. Error bars depict standard deviation.

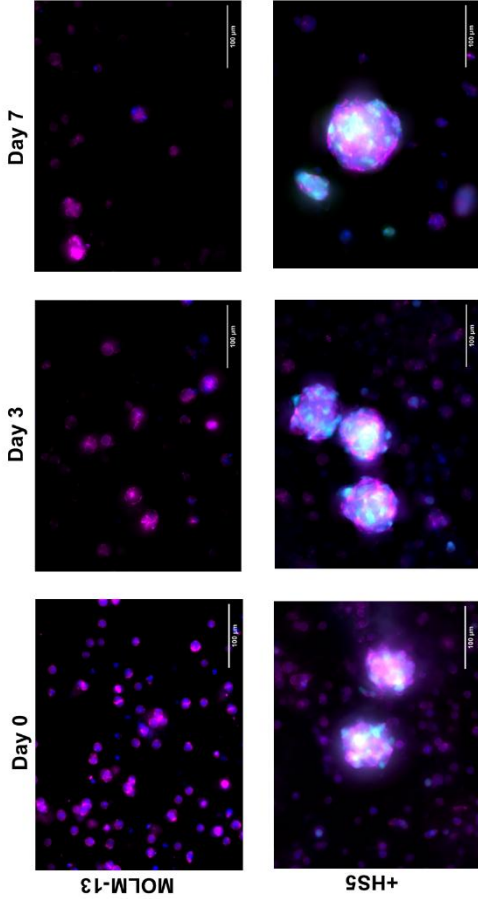
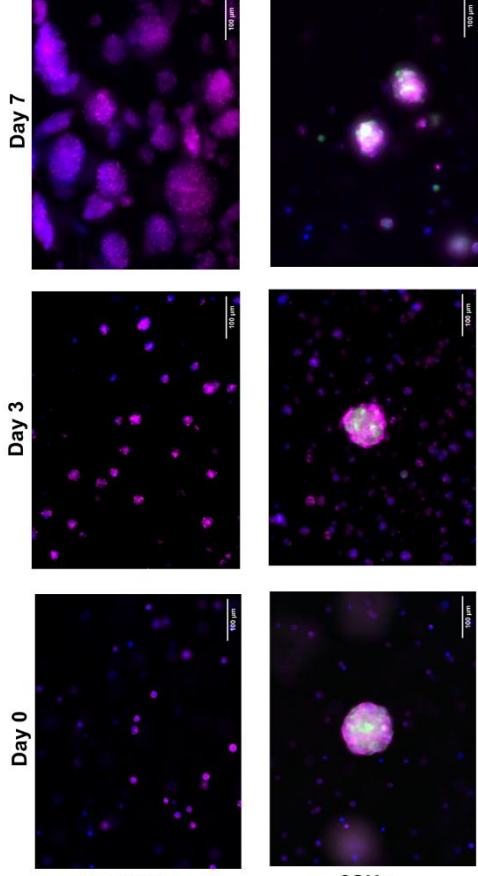
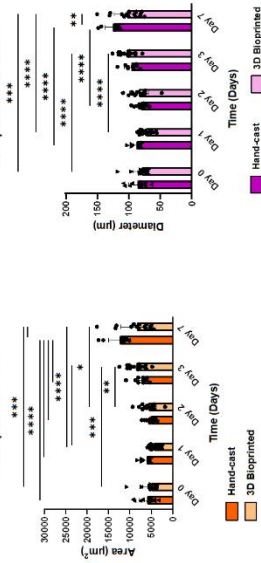
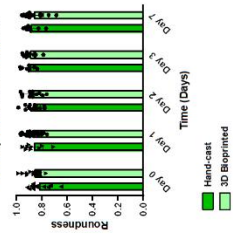
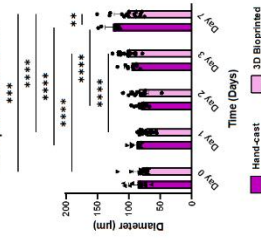
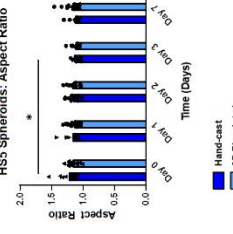
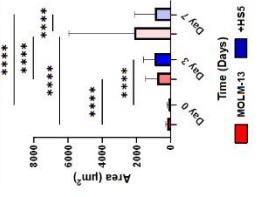
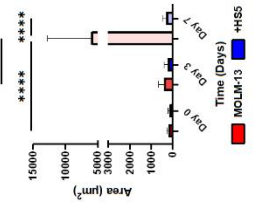


**Supplementary Figure 3: Diffusion of fluorescent nanoparticles through 2%Alg 8%Gel hand-cast hydrogels to simulate diffusion of chemotherapeutic drugs.** Hydrogels were submerged in DMEM containing FluorMag nanoparticles conjugated to FITC at 200  $\mu\text{g}/\text{mL}$  and imaged at regular intervals over 24 hours. Here, it shows that small particles can diffuse through the hydrogels after at least two hours. Images were taken using a Zeiss Axiovert microscope at 5X, with the FITC channel exposure set at 800 ms across all timepoints.



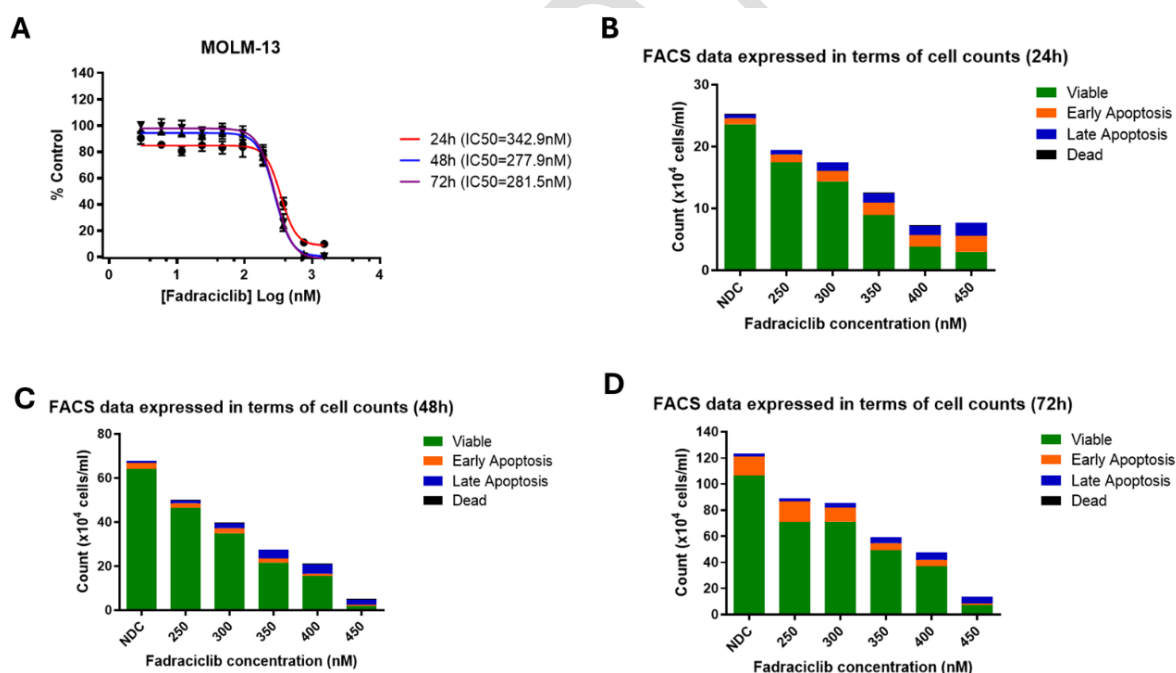
bioRxiv preprint doi: <https://doi.org/10.1101/2023.08.15.552888>; this version posted August 15, 2023. The copyright holder for this preprint (which was not certified by peer review) is the author/funder, who has granted bioRxiv a license to display the preprint in perpetuity. It is made available under aCC-BY-NC-ND 4.0 International license.

**Supplementary Figure 4: Viability MOLM-13 cells and HS5 spheroids within hand-cast and 3D bioprinted 2%Alg 8%Gel hydrogels.** A: MOLM-13 cells in monoculture and co-cultured with GFP-HS5 spheroids within hand-cast 2%Alg 8%Gel hydrogels stained with live/dead stain; B: 3D bioprinted alginate/gelatin hydrogels containing MOLM-13 cells in monoculture and co-cultured with GFP-HS5 spheroids stained with live/dead stain (20X magnification; scale bar: 100  $\mu$ m); C: Comparison of monoculture MOLM-13 viability in hand-cast and 3D bioprinted alginate/gelatin gels; D: Comparison of co-cultured MOLM-13 cell viability in hand-cast and 3D bioprinted alginate/gelatin gels; E: Comparison of MOLM-13 monoculture and HS5 co-culture viability. Green: HS5 cells (GFP-HS5 cells); blue: live cells; red: dead cells; F: Comparison of HS5 spheroid viability in hand-cast and 3D bioprinted hydrogels for up to seven days. HS5 spheroid viability was calculated using the JACOP plugin on Fiji, whereby the Mandler's coefficient was used to determine the degree of overlap of GFP (green channel) with either live (blue channel) or dead (red channel). Hand-cast viability images were taken using Zeiss Axiovert microscope, and 3D bioprinted viability images were taken using the EVOS M7000 Imager. Single plane images were taken at 10X for analysis and 20X for representative images. One-way ANOVAs with multiple comparisons were used in C-F. Significance is shown using asterisks, and an absence of this indicates a lack of significance. Significance: \*  $P \leq 0.05$ ; \*\*  $P \leq 0.01$ ; \*\*\*  $P \leq 0.001$  \*\*\*\*  $P \leq 0.0001$ . Bars represent the average of nine technical replicates (three images per hydrogel, total of nine datapoints) with standard deviation shown as error bars.

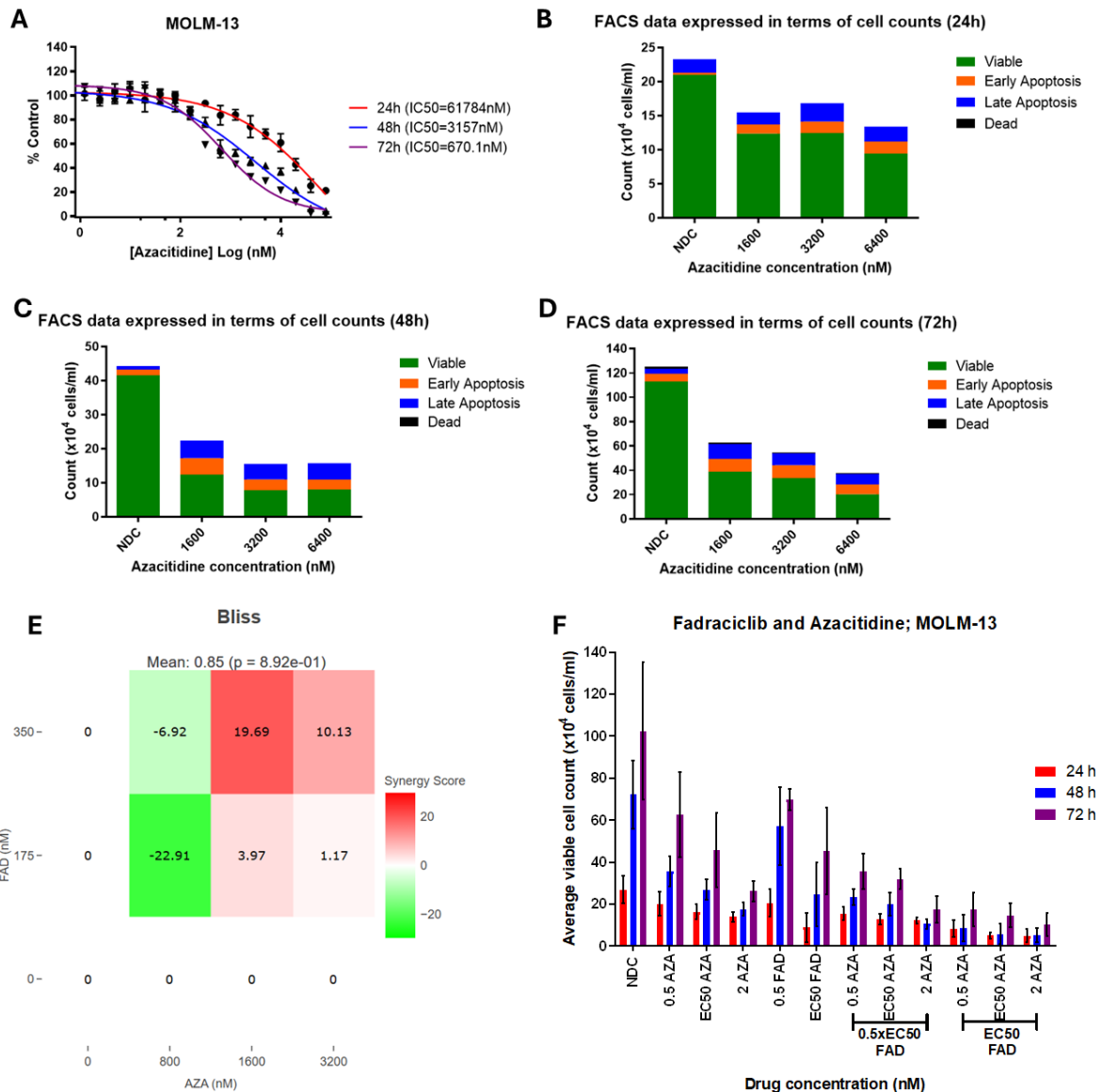
**A****Hand-cast****B****3D Bioprinted****C****Hand-cast and 3D Bioprinted HS5 Spheroids: Area****E****Hand-cast and 3D Bioprinted HS5 Spheroids: Roundness****D****Hand-cast and 3D Bioprinted HS5 Spheroids: Diameter****F****Hand-cast and 3D Bioprinted HS5 Spheroids: Aspect Ratio****G****Hand-cast MOLM-13 cell cluster area****H****3D Bioprinted MOLM-13 cell cluster area**

ER

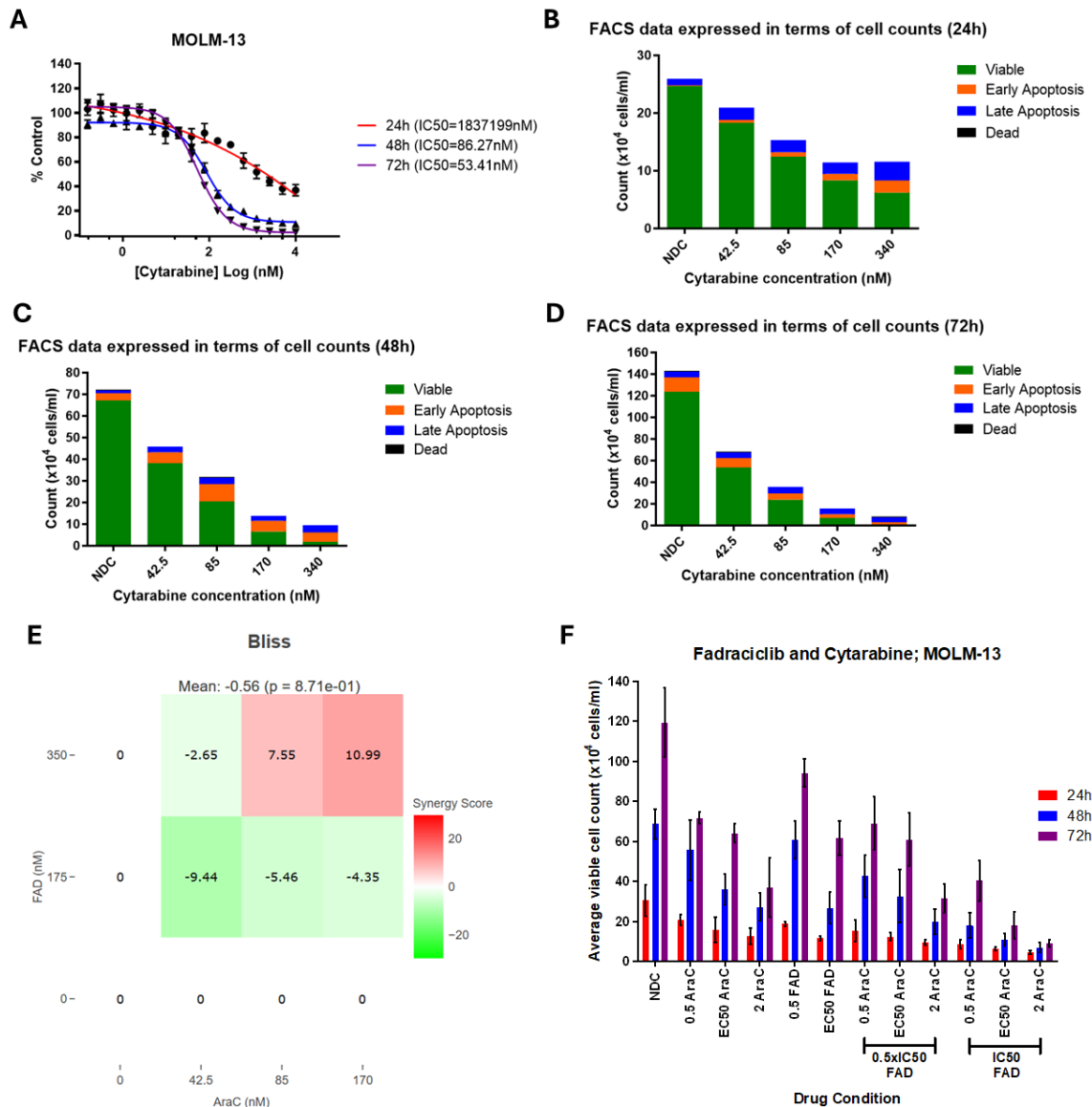
**Supplementary Figure 5: Morphology of MOLM-13 cells within hand-cast and 3D bioprinted 2%Alg 8%Gel hydrogels.** A: Representative images of MOLM-13 cells in monoculture and co-cultured with GFP-HS5 spheroids within hand-cast 2%Alg 8%Gel hydrogels stained for F-Actin and DAPI nuclear stain (20X magnification; scale bar: 100  $\mu$ m); B: MOLM-13 cells in monoculture and co-cultured with GFP-HS5 spheroids within 3D bioprinted 2%Alg 8%Gel hydrogels stained for F-Actin and DAPI nuclear stain (20X magnification; scale bar: 100  $\mu$ m). Green: HS5 cells; blue: DAPI (Nuclei); magenta: F-Actin. Spheroids were quantified for hand-cast and 3D bioprinted spheroids and area (C), diameter (D), roundness (E), and aspect ratio (F) are depicted as bar charts. The cluster size of MOLM-13 cells in monoculture and HS5 co-culture in hand-cast (G) and 3D bioprinted (H) hydrogels were quantified using Fiji and shown as bar charts. Analyses were completed using images taken at 10X magnification. Representative z-stack images were taken at 20X magnification, and the Maximal Intensity Projection was selected to produce the final images. Hand-cast hydrogel images were taken using Zeiss Axiovert microscope, and 3D bioprinted images were taken using the EVOS M7000 Imager. One-way ANOVAs with multiple comparisons were used in C-H to detect significant differences between conditions. Significance is shown using asterisks, and an absence of this indicates a lack of significance. Significance: \*  $P \leq 0.05$ ; \*\*  $P \leq 0.01$ ; \*\*\*  $P \leq 0.001$  \*\*\*\*  $P \leq 0.0001$ . Bars represent the average of nine technical replicates (three images per hydrogel, total of nine datapoints) with standard deviation shown as error bars.



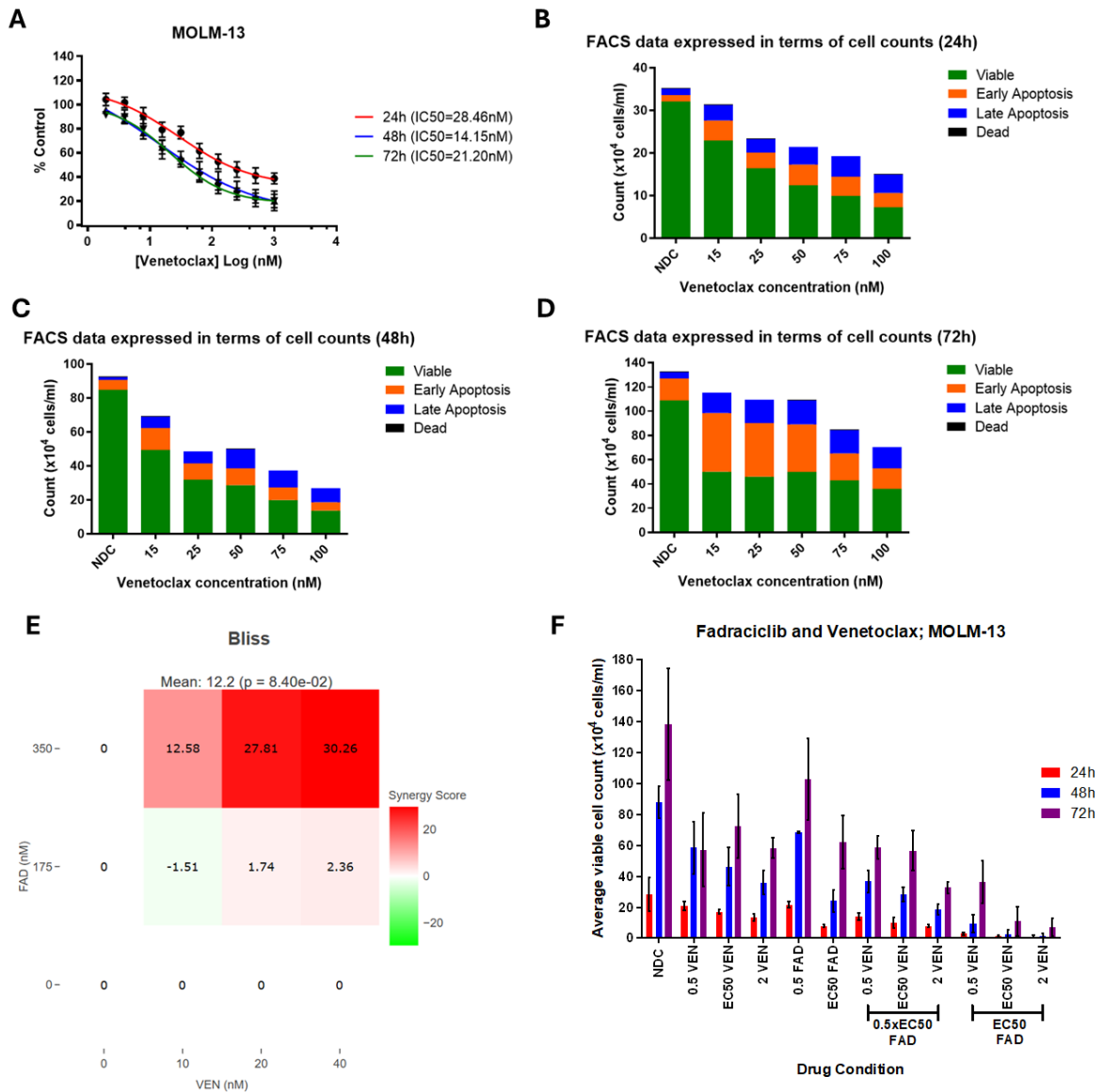
**Supplementary Figure 6: Determining the EC50 of fadraciclib (FAD) on MOLM-13 cells.** The cells were treated with fadraciclib in a range of 250-450 nM and analysed after 24, 48 and 72 hours. A: Logarithmic graph depicting the results of the resazurin reduction assays (n=3) at 24h (red), 48h (blue), and 72h (purple). N=3. Error bars depict standard deviation. B-D: Annexin V/DAPI data expressed in terms of absolute cell counts per condition at 24, 48 and 72 hours (respectively). Viable (green – Annexin V negative, DAPI negative), Early Apoptosis (orange – Annexin V positive, DAPI negative), Late Apoptosis (orange – Annexin V positive, DAPI positive), Dead (orange – Annexin V negative, DAPI positive). N=1.



**Supplementary Figure 7: Determining the EC50 of azacitidine (AZA) on MOLM-13 cells and optimal combination with fadraciclib.** The concentrations used were 1600 nM, 3200 nM and 6400 nM (0.5x EC50, EC50 and 2xEC50 from 48 hours resazurin assay). A: Logarithmic graph showing the results of the resazurin assays (n=3) at 24h (red), 48h (blue), and 72h (purple). B-D: Annexin V/DAPI data expressed in terms of absolute cell counts per condition at 24, 48 and 72 hours (respectively). E: Heatmap displaying the synergy calculated for each dosage combination using the Bliss Independence model at 48h. Heatmap produced using Synergy Finder+ software<sup>1</sup>. F: A bar chart depicting all fadraciclib and azacitidine combinations assessed on MOLM-13 cells. The cell numbers were calculated using trypan blue staining and the proportion of viable cells were taken from Annexin V/DAPI staining. FAD EC50: 350 nM, AZA EC50: 1600 nM. 24h: Red, 48h: blue, 72h: purple. Bars represent the average of three biological replicates with standard deviation depicted as error bars.

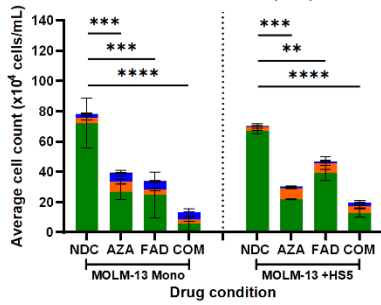


**Supplementary Figure 8: Determining the EC<sub>50</sub> of cytarabine (AraC) on MOLM-13 cells and dose optimisation with fadraciclib.** A: Logarithmic graph displaying the results of the resazurin assays (n=3) at 24h (red), 48h (blue), and 72h (purple). B-D: Annexin V/DAPI data expressed in terms of absolute cell counts per condition at 24, 48 and 72 hours (respectively). The cells were treated with 42.5 nM, 85 nM, 170 nM and 340 nM (0.5x EC<sub>50</sub>, EC<sub>50</sub>, 2xEC<sub>50</sub> and 4xEC<sub>50</sub> from 48h resazurin). E: Heatmap displaying the synergy calculated for each dosage combination using the Bliss Independence model at 48h. Heatmap produced using Synergy Finder+ software<sup>1</sup>. F: A bar chart depicting all fadraciclib and cytarabine combinations assessed on MOLM-13 cells. The cell numbers were calculated using trypan blue staining and the proportion of viable cells were taken from Annexin V/DAPI staining. FAD EC<sub>50</sub>: 350 nM, AraC EC<sub>50</sub>: 42.5 nM. 24h: Red, 48h: blue, 72h: purple. Bars represent the average of three biological replicates with standard deviation depicted as error bars.

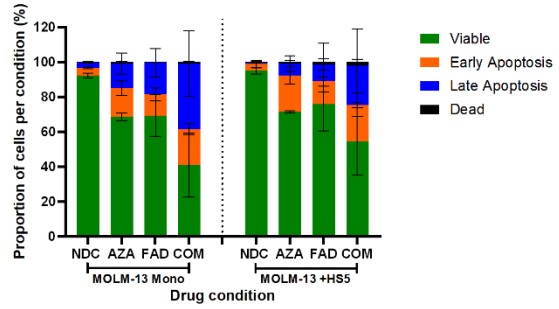


**Supplementary Figure 9: Determining the EC50 of venetoclax (VEN) and the optimal combination of venetoclax and fadraciclib on MOLM-13 cells.** A: Logarithmic graph displaying the results of the resazurin reduction assays ( $n=3$ ) at 24h (red), 48h (blue), and 72h (purple). B-D: Annexin V/DAPI data expressed as absolute cell counts per condition at 24, 48 and 72 hours (respectively). E: Heatmap displaying the synergy calculated for each dosage combination using the Bliss Independence model at 48h. Heatmap produced using Synergy Finder+ software<sup>1</sup>. F: A bar chart depicting all fadraciclib and venetoclax combinations assessed on MOLM-13 cells. The cell numbers were calculated using trypan blue staining and the proportion of viable cells were taken from Annexin V/DAPI staining. Due to the potency of these combinations, the 0.5 $\times$ IC50 values of fadraciclib and venetoclax were selected (FAD 0.5 $\times$ EC50: 175 nM, VEN 0.5 $\times$ EC50: 10 nM). 24h: Red, 48h: blue, 72h: purple. Bars represent the average of three biological replicates with standard deviation depicted as error bars.

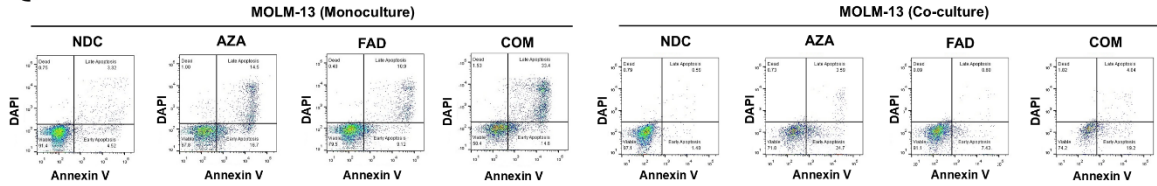
**A** Annexin V/DAPI data in terms of viable cell count; Fadracliclib and Azacitidine (48h); MOLM-13



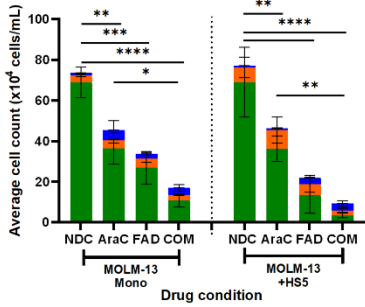
**B** Annexin V/DAPI Apoptosis Assay; Fadracliclib and Azacitidine (48h); MOLM-13



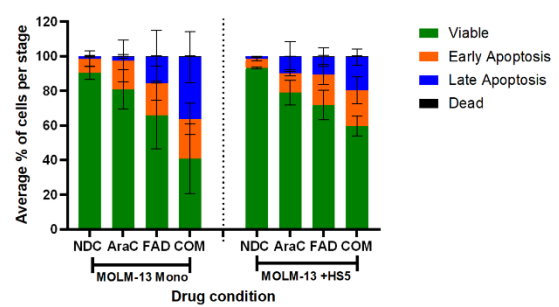
**C**



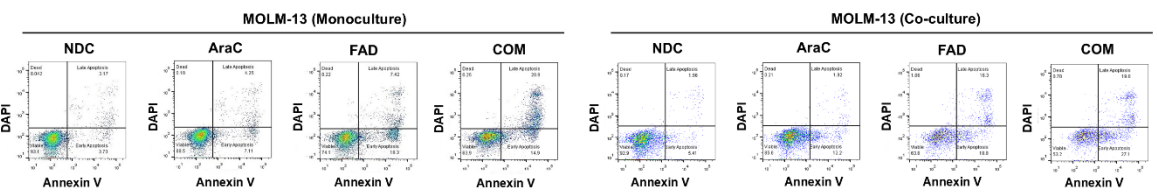
**D** Annexin V/DAPI data in terms of viable cell count; Fadracliclib and Cytarabine (48h); MOLM-13



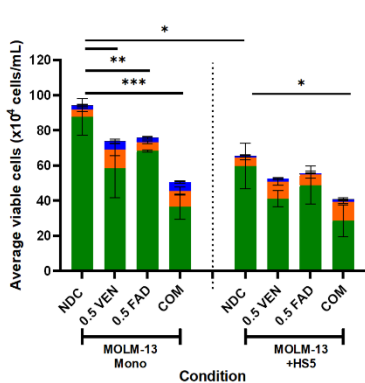
**E** Annexin V/DAPI Apoptosis Assay; Fadracliclib and Cytarabine (48h); MOLM-13



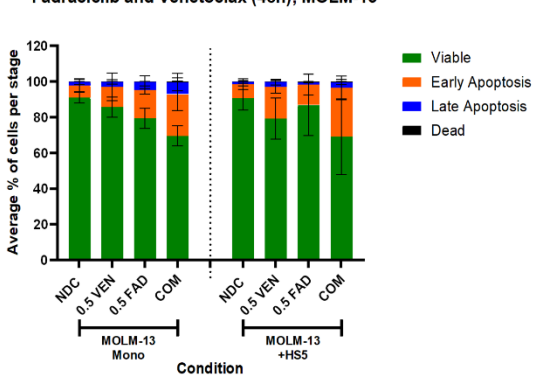
**F**



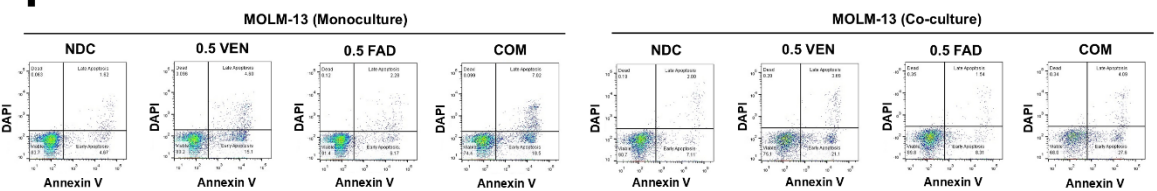
**G** Annexin V/DAPI data in terms of viable cell count; Fadracliclib and Venetoclax (48h); MOLM-13



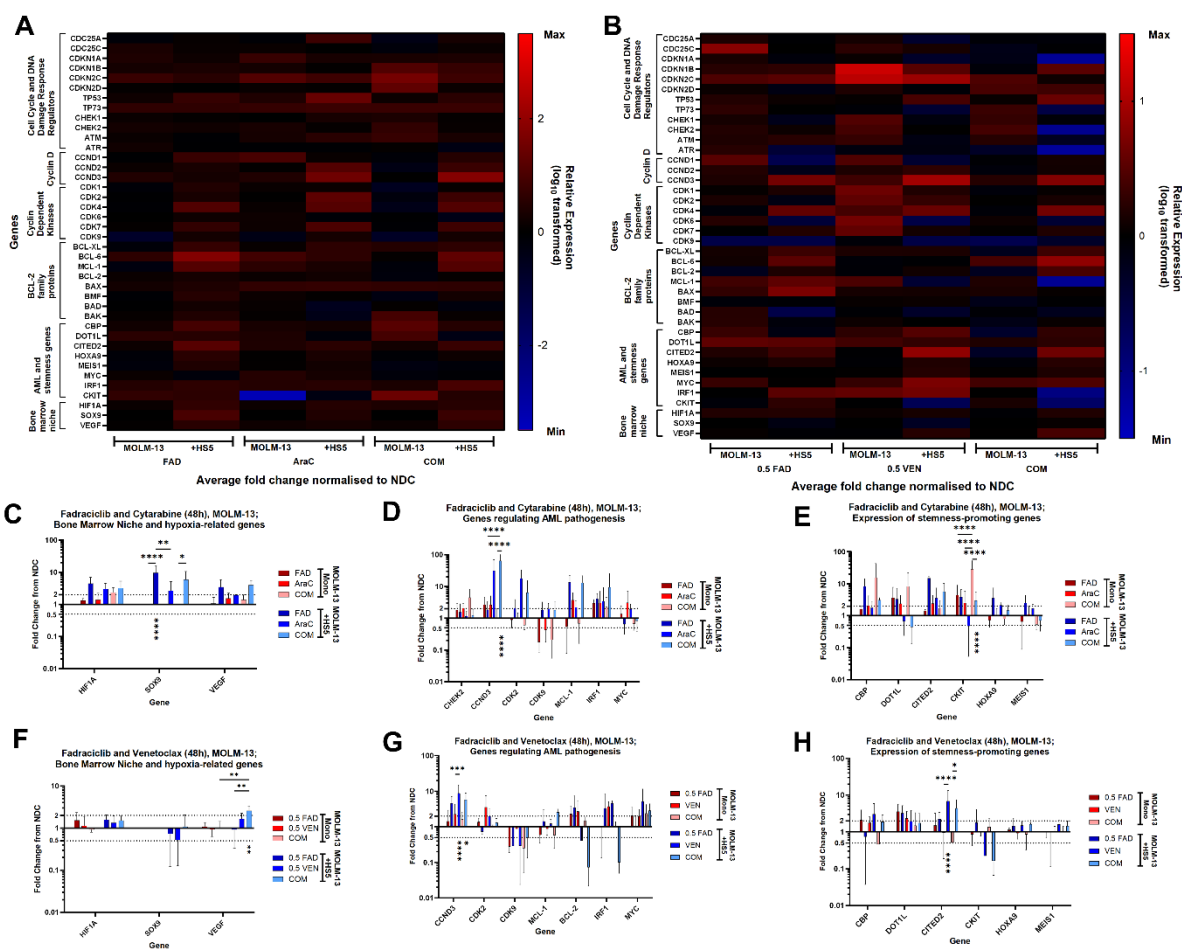
**H** Annexin V/DAPI Apoptosis Assay; Fadracliclib and Venetoclax (48h); MOLM-13



**I**

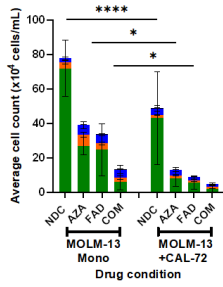


**Supplementary Figure 10: MOLM-13 cells in 2D monoculture and HS5 co-culture treated with fadraciclib and current AML therapies.** A, D, G: Annexin V/DAPI data shown in terms of cell counts for MOLM-13 cells treated with fadraciclib (FAD) alone, in combination with azacitidine (AZA; A), cytarabine (AraC; D) or venetoclax (VEN; G) and combination (COM) therapy in monoculture and co-culture. B, E, H: Bar chart showing the proportion of cells in each apoptotic stage through Annexin V/DAPI apoptosis staining for FAD alone and in combination with AZA (B), AraC (E), or VEN (H). A one-way ANOVA was used to detect significant differences between conditions in B, E, H. C, F, I: Representative Annexin V/DAPI scatter plots showing the proportions of NDC and drug treated MOLM-13 cells in monoculture (left) and co-culture (right) in each stage of apoptosis 48 hours post treatment. Significance: \*  $P \leq 0.05$ ; \*\*  $P \leq 0.01$ ; \*\*\*  $P \leq 0.001$  \*\*\*\*  $P \leq 0.0001$ . Bars represent the mean of three biological replicates, and standard deviation depicted as error bars.

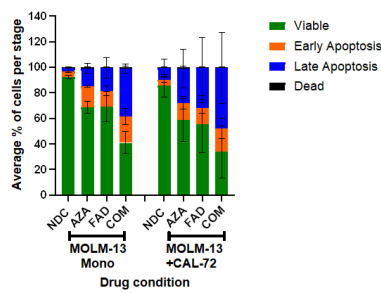


**Supplementary Figure 11: The effect of fadraciclib alone and combination with cytarabine and venetoclax on MOLM-13 gene expression.** A, B: Heat maps displaying differences in gene expression for MOLM-13 cells in monoculture and HS5 co-culture following treatment with fadraciclib (FAD) alone and in combination with cytarabine (AraC, A) or venetoclax (VEN, B), normalised to NDC. Blue: downregulated compared to NDC; red: upregulated. C, F: bone marrow niche and hypoxia-related gene expression after treatment with cytarabine (C) and venetoclax (F); D, G: expression of genes regulating AML pathogenesis after cytarabine (D) and venetoclax (G) treatments; E, H: stemness-promoting gene expression after cytarabine (E) and venetoclax (H) single and combination treatments. Two-way ANOVAs with multiple comparisons were used to detect significant differences between conditions in B, C, E, F. Significance: \*  $P \leq 0.05$ ; \*\*  $P \leq 0.01$ ; \*\*\*  $P \leq 0.001$  \*\*\*\*  $P \leq 0.0001$ . Bars represent the mean of three biological replicates, and standard deviation depicted as error bars.

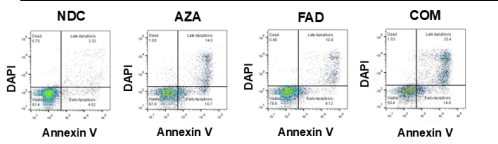
**A** Annexin V/DAPI data in terms of viable cell count; Fadcriclib and Azacitidine (48h); MOLM-13 (CAL-72 Co-Culture)



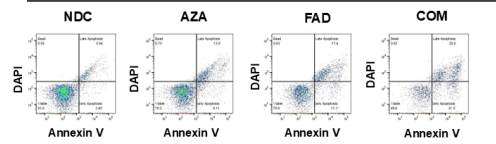
**B** Annexin V/DAPI Apoptosis Assay; Fadcriclib and Azacitidine (48h); MOLM-13 (CAL-72 Co-Culture)



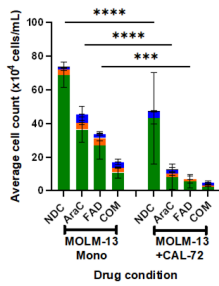
**C** MOLM-13 (Monoculture)



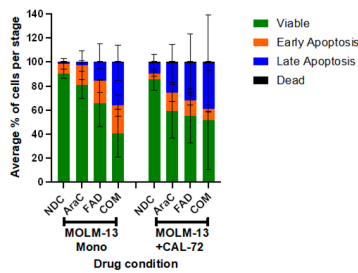
MOLM-13 (CAL-72 Co-Culture)



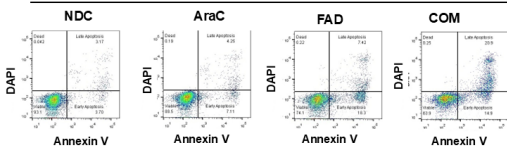
**D** Annexin V/DAPI data in terms of viable cell count; Fadcriclib and Cytarabine (48h); MOLM-13 and MOLM-13/CAL-72 Co-Culture



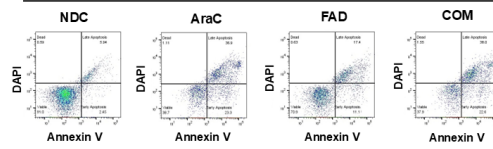
**E** Annexin V/DAPI Apoptosis Assay; Fadcriclib and Cytarabine (48h); MOLM-13 (CAL-72 Co-Culture)



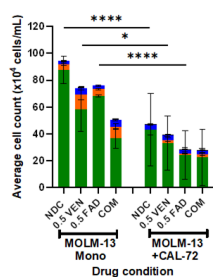
**F** MOLM-13 (Monoculture)



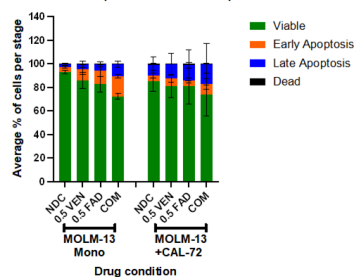
MOLM-13 (CAL-72 Co-Culture)



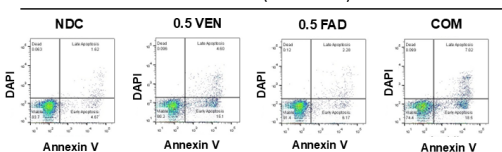
**G** Annexin V/DAPI data in terms of viable cell count; Fadcriclib and Venetoclax (48h); MOLM-13 and MOLM-13/CAL-72 Co-Culture



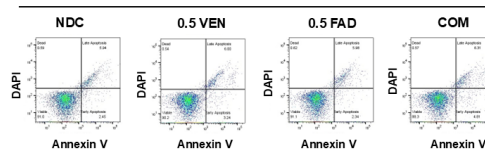
**H** Annexin V/DAPI Apoptosis Assay; Fadcriclib and Venetoclax (48h); MOLM-13 (CAL-72 Co-Culture)



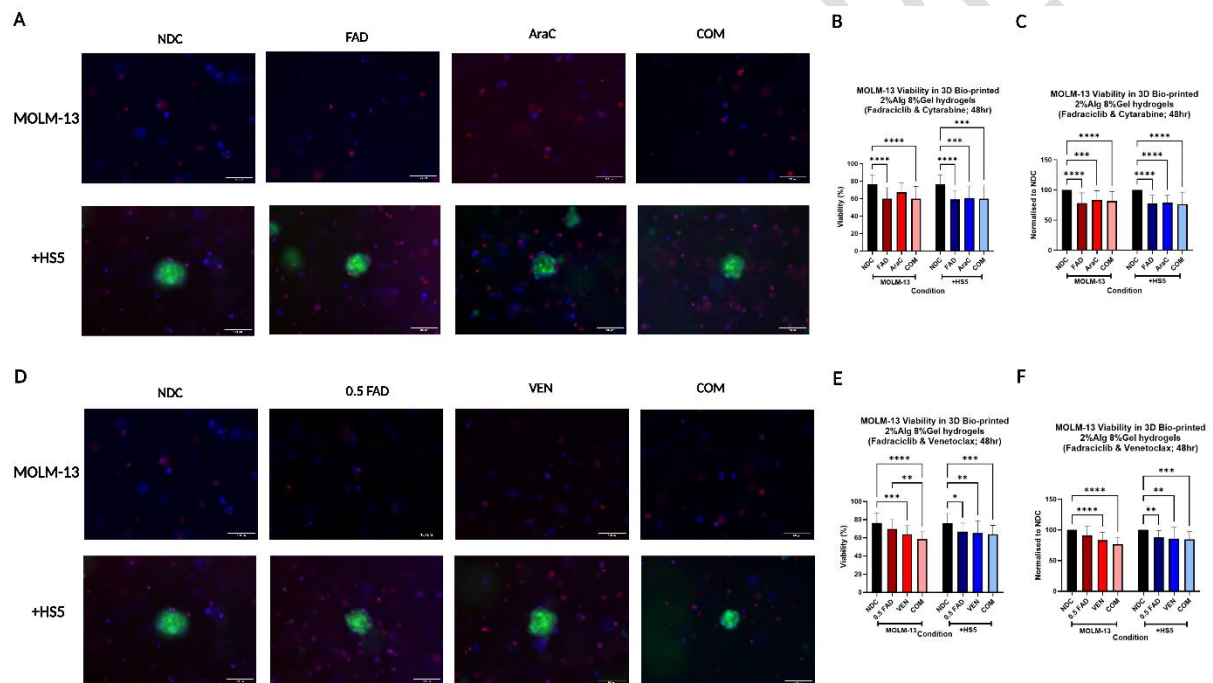
**I** MOLM-13 (Monoculture)



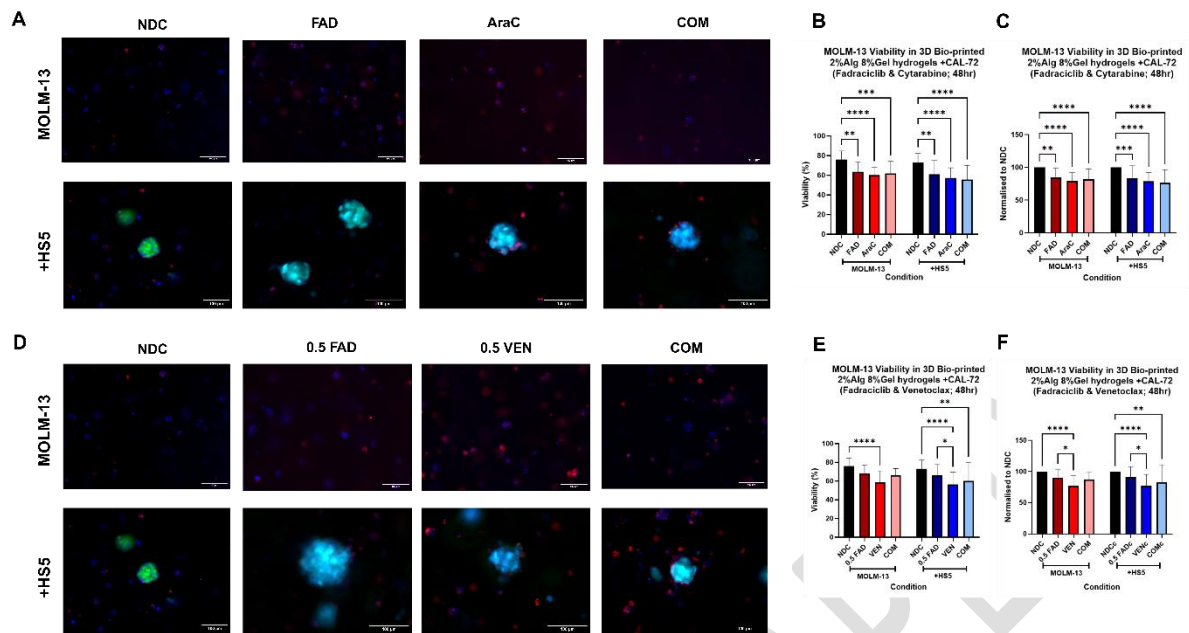
MOLM-13 (CAL-72 Co-Culture)



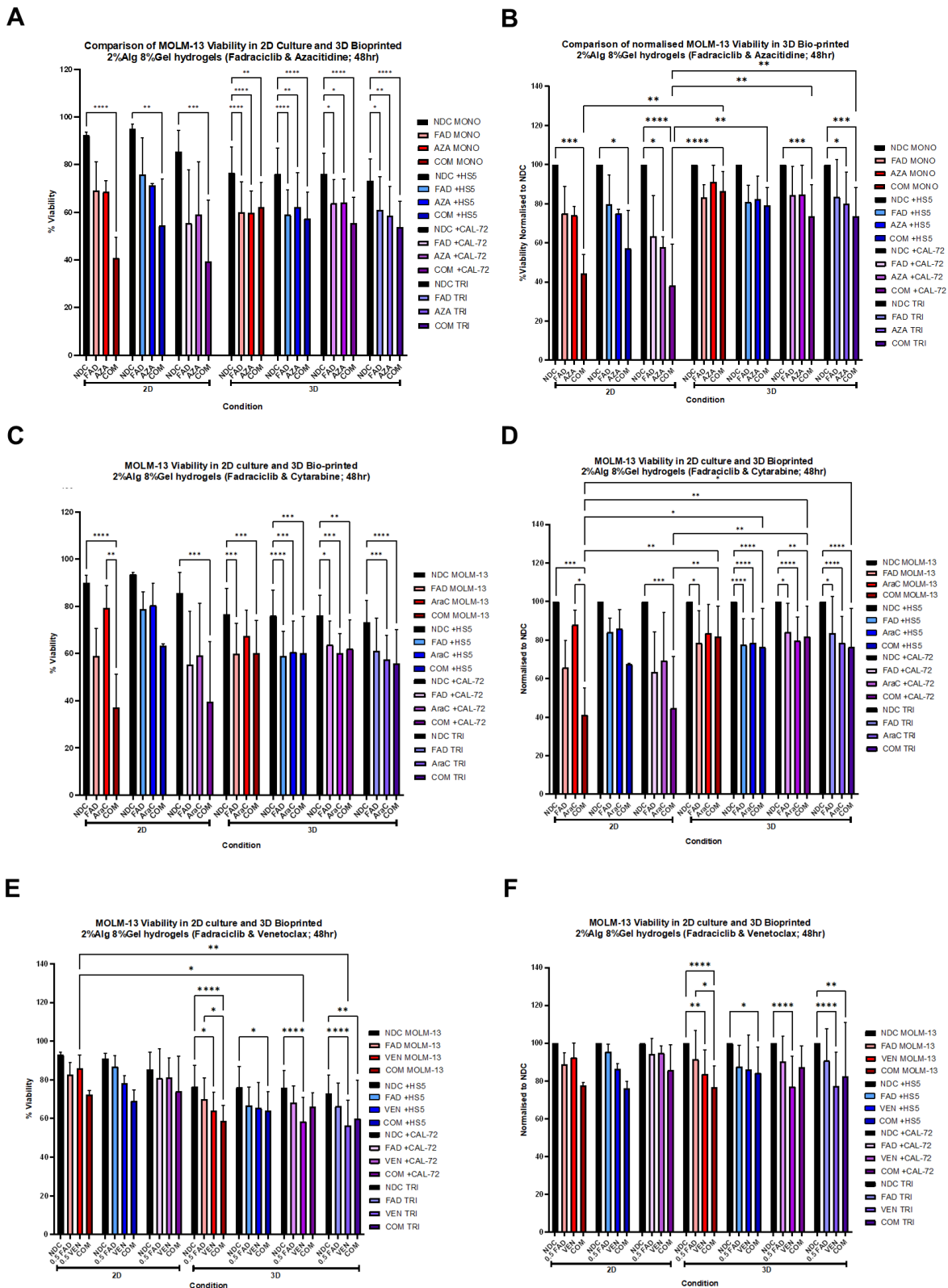
**Supplementary Figure 12: MOLM-13 cells in 2D monoculture and CAL-72 co-culture treated with fadraciclib and selected AML therapies.** A, D, G: Annexin V/DAPI data shown in terms of cell counts for MOLM-13 cells treated with fadraciclib (FAD), azacitidine (AZA; A), cytarabine (AraC; D) or venetoclax (VEN; G) and combination (COM) therapies of fadraciclib with these drugs in monoculture and CAL-72 co-culture. B, E, H: Bar chart showing the proportion of cells in each apoptotic stage through Annexin V/DAPI apoptosis staining for FAD alone and in combination with AZA (B), AraC (E), or VEN (H) in monoculture and CAL-72 co-culture. A one-way ANOVA was used to detect significant differences between conditions in B, E, H. C, F, I: Representative Annexin V/DAPI scatter plots showing the proportions of NDC and drug treated MOLM-13 cells in monoculture (left) and CAL-72 co-culture (right) in each stage of apoptosis. Significance: \*  $P \leq 0.05$ ; \*\*  $P \leq 0.01$ ; \*\*\*  $P \leq 0.001$  \*\*\*\*  $P \leq 0.0001$ . Bars represent the mean of three biological replicates, and standard deviation depicted as error bars.



**Supplementary Figure 13: MOLM-13 cells in 3D monoculture and HS5 spheroid co-culture treated with fadraciclib with cytarabine or venetoclax.** A, D: Representative images of 3D bioprinted MOLM-13 cells in monoculture and HS5 spheroid co-culture 48 hours after treatment with fadraciclib (FAD), cytarabine (AraC), venetoclax (VEN) or a combination of FAD with AraC or VEN (COM). Images taken at 20X using the M7000 Imager (scale bar 100  $\mu\text{m}$ ). Green: HS5 cells (GFP-HS5 cells); blue: live cells; red: dead cells. B, E: MOLM-13 cell viability within 3D bioprinted 2%Alg 8%Gel hydrogels following drug treatment. C, F: MOLM-13 cell viability normalised to NDC. One-way ANOVAs with multiple comparisons were used to find significant differences between conditions in B, C, E, F. Significance: \*  $P \leq 0.05$ ; \*\*  $P \leq 0.01$ ; \*\*\*  $P \leq 0.001$  \*\*\*\*  $P \leq 0.0001$ . Bars represent the mean of three biological replicates, and standard deviation depicted as error bars.



**Supplementary Figure 14: Assessment of fadraciclib with cytarabine or venetoclax within the final 3D bioprinted model.** A, D: Representative images of the final 3D bioprinted AML model, comprising MOLM-13 cells in monoculture and HS5 spheroid co-culture cultured with a CAL-72 monolayer. Images taken 48 hours after treatment with fadraciclib (FAD), cytarabine (AraC), venetoclax (VEN) or a combination of FAD with AraC or VEN (COM). Images taken at 20X using the M7000 Imager (scale bar 100  $\mu$ m). Green: HS5 cells (GFP-HS5 cells); blue: live cells; red: dead cells. B, E: MOLM-13 cell viability within 3D bioprinted 2%Alg 8%Gel hydrogels following drug treatment. C, F: MOLM-13 cell viability normalised to NDC. One-way ANOVAs with multiple comparisons were used to find significant differences between conditions in B, C, E, F. Significance: \*  $P \leq 0.05$ ; \*\*  $P \leq 0.01$ ; \*\*\*  $P \leq 0.001$  \*\*\*\*  $P \leq 0.0001$ . Bars represent the mean of three biological replicates, and standard deviation depicted as error bars.

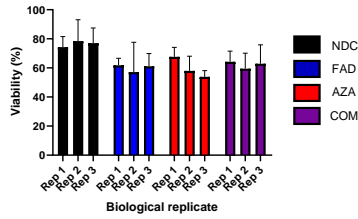


**Supplementary Figure 15: Bar charts comparing all conditions assessed within this study for fadraciclib in combination with azacitidine, cytarabine and venetoclax. A, C, E: MOLM-13 viability after treatment with fadraciclib (FAD), azacitidine (AZA; A), cytarabine (AraC, C) and venetoclax (VEN, E) in all 2D and 3D conditions. B, D, F: MOLM-13 cell viability normalised to NDC following treatment with FAD and AZA (B), AraC (D) and VEN (F). One-way ANOVAs with multiple comparisons were used to detect significant differences**

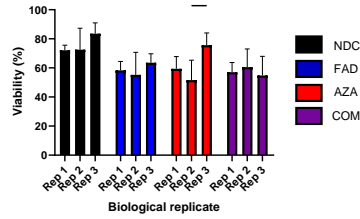
between conditions. Significance: \*  $P \leq 0.05$ ; \*\*  $P \leq 0.01$ ; \*\*\*  $P \leq 0.001$  \*\*\*\*  $P \leq 0.0001$ . Bars represent the average of three biological replicates with standard deviation shown as error bars.

ACCEPTED PAPER

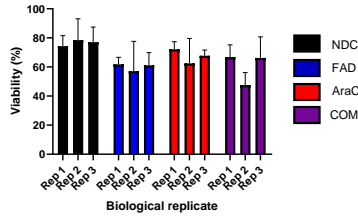
**A** Monoculture MOLM-13 Viability in 3D Bio-printed 2%Alg 8%Gel hydrogels (Fadraciclib & Azacitidine; 48hr)



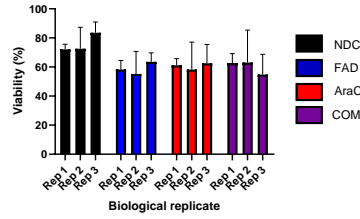
**B** Co-culture MOLM-13 Viability in 3D Bio-printed 2%Alg 8%Gel hydrogels (Fadraciclib & Azacitidine; 48hr)



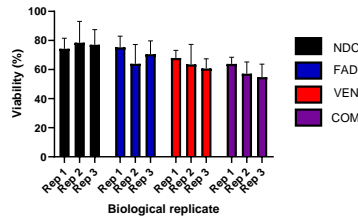
**C** Monoculture MOLM-13 Viability in 3D Bio-printed 2%Alg 8%Gel hydrogels (Fadraciclib & Cytarabine; 48hr)



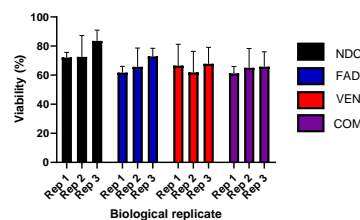
**D** Co-culture MOLM-13 Viability in 3D Bio-printed 2%Alg 8%Gel hydrogels (Fadraciclib & Cytarabine; 48hr)



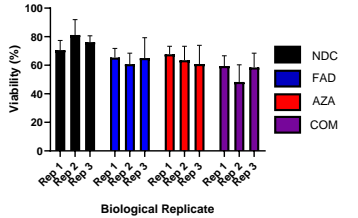
**E** Monoculture MOLM-13 Viability in 3D Bio-printed 2%Alg 8%Gel hydrogels (Fadraciclib & Venetoclax; 48hr)



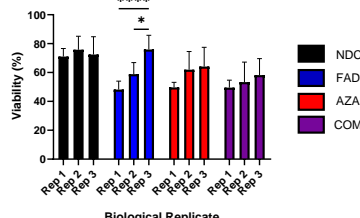
**F** Co-culture MOLM-13 Viability in 3D Bio-printed 2%Alg 8%Gel hydrogels (Fadraciclib & Venetoclax; 48hr)



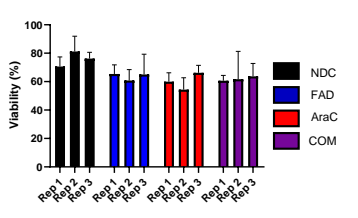
**G** MOLM-13 Viability in 3D Bioprinted 2%Alg 8%Gel hydrogels (CAL-72 Co-Culture) (Fadraciclib & Azacitidine; 48hr)



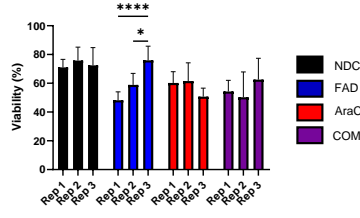
**H** MOLM-13 Viability in 3D Bioprinted 2%Alg 8%Gel hydrogels (HS5 spheroid, CAL-72 Co-Culture) (Fadraciclib & Azacitidine; 48hr)



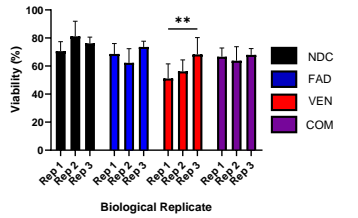
**I** MOLM-13 Viability in 3D Bioprinted 2%Alg 8%Gel hydrogels (CAL-72 Co-Culture) (Fadraciclib & Cytarabine; 48hr)



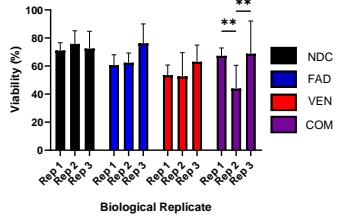
**J** MOLM-13 Viability in 3D Bioprinted 2%Alg 8%Gel hydrogels (HS5 spheroid, CAL-72 Co-Culture) (Fadraciclib & Cytarabine; 48hr)



**K** MOLM-13 Viability in 3D Bioprinted 2%Alg 8%Gel hydrogels (CAL-72 Co-Culture) (Fadraciclib & Venetoclax; 48hr)



**L** MOLM-13 Viability in 3D Bioprinted 2%Alg 8%Gel hydrogels (HS5 spheroid, CAL-72 Co-Culture) (Fadraciclib & Venetoclax; 48hr)



**Supplementary figure 16: Assessing inter-replicate variability in 3D bioprinted MOLM-13 cells treated with selected chemotherapies.** Each biological replicate was compared to the other biological replicates (n=9 technical replicates each) to assess whether the results obtained from the intermediate 3D model (A-F, no CAL-72 monolayer) and the final 3D model (G-L, with CAL-72 monolayer) were reproducible across experiments. One Way ANOVAs with multiple comparisons were completed to detect significant differences. Overall, few significant differences were found between replicates, highlighting that this model is highly reproducible. Significance: \*  $P \leq 0.05$ ; \*\*  $P \leq 0.01$ ; \*\*\*  $P \leq 0.001$  \*\*\*\*  $P \leq 0.0001$ . Bars represent the mean of three biological replicates, and standard deviation depicted as error bars. Rep: replicate. FAD: fadraciclib. AZA: azacitidine. AraC: cytarabine. VEN: venetoclax. COM: combination therapy of fadraciclib plus the additional selected chemotherapy in each graph.

**Supplementary Table 1: A table summarising the drug concentrations which induce 50% apoptosis in MOLM-13 cells.**

Drug (nM)	24h	48h	72h
Fadraciclib	350	350	350
Azacitidine	6400	1600	1600
Cytarabine	85	85	42.5
Venetoclax	25	20	15

Notes: These concentration ranges were estimated using resazurin assays and determined using Annexin V/DAPI staining and trypan blue exclusion staining. Concentrations measured in nM.

**Supplementary Table 2: Primers selected for multiplex qRT-PCR.**

<b>Primer</b>	<b>Gene</b>	<b>Forward (5'to3')</b>	<b>Reverse (5'to3')</b>
<b>ATM</b>	Ataxia-Telangiectasia Mutated	CGGAGCTGATTGTAGCAACATACTA	CAGATAGAGCCTGAAGTACACAGAG
<b>ATP5B</b>	ATP synthase F1 subunit beta	TCCATCCTGTCAGGGACTATG	ATCAAACCTGGACGTCCACCAC
<b>ATR</b>	Ataxia Telangiectasia and Rad3-related	CAGCTCTCTATGAAGGCCATTC	GTTCTACTGTTTCACTGTCTGTTGC
<b>B2M</b>	beta-2 microglobulin	GTCTTTCAGCAAGCACTGGTCT	CTTAGATGTCTCGATCCCACCTT
<b>BAD</b>	BCL2 Associated Agonist Of Cell Death	CTTTAAGAAGGGACTTCCTCGC	CAAGTTCGGATCCCACCAGG
<b>BAK</b>	BCL2 Antagonist/Killer 1	TCATCGGGGACGACATCAAC	CAAACAGGCTGGTGGCAATC
<b>BAX</b>	BCL2-associated X protein	GACATTGGACTTCCTCCGGG	ACAGGGACATCAGTCGCTTC
<b>BCL2</b>	B-cell CLL/lymphoma 2	CCCTGTGGATGACTGAGTACC	GTTCCACAAAGGCATCCCAGC
<b>BCL6</b>	B-cell lymphoma 6	GCACTTGGGACCACAGAGAAA	ATGCCTTGCTTCACAGTCCA
<b>BCLXL</b>	B-cell lymphoma extra large	AGCTGGTTTTTTTGGCCAGCC	TCTCTTCTAAGATCCAAAGCC
<b>BMF</b>	Bcl-2-modifying factor	GAACCCAGCGACTCTTTTA	TTTCGGGCAATCTGTACCTC
<b>CBP</b>	CREB-binding protein	TTCTTCCCGGAGACTGAGGT	GACAGGGAGGATGGAGGAGT
<b>CCND1</b>	Cyclin D1	GATCAAGTGTGACCCGGACTG	CCTTGGGGTCCATGTTCTGC
<b>CCND2</b>	Cyclin D2	CACCAACACAGACGTGGATTG	CTCCGACTTGGATCCGTCAC
<b>CCND3</b>	Cyclin D3	CAGAGCCTGCTCCGCC	CTGCTCCTCACATACCTCCA
<b>CDC25A</b>	Cell Division Cycle 25A	GTCTAGATTCTCCTGGGCCATT	CAGAATGGCTCCTCTTCAGAGC
<b>CDC25B</b>	Cell Division Cycle 25B	GTTTGTGGCTGCCCTGC	CGACAGGGAGGATTCGGATG
<b>CDC25C</b>	Cell Division Cycle 25C	AATGTAGCCCAGCACAGCTT	GTAAGGCAGCCACCTTGAA
<b>CDKI</b>	Cyclin Dependent Kinase 1	ATGAAGTGTGGCCAGAAGTG	CAGAAATTCGTTTGGCTGGATCA

<b>CDK2</b>	Cyclin Dependent Kinase 2	GCTTGTTATCGCAAATGCTGC	GATGGGGTACTGGCTTGGTC
<b>CDK4</b>	Cyclin Dependent Kinase 4	GAAACTCTGAAGCCGACCAG	AGGCAGAGATTCGCTTGTGT
<b>CDK6</b>	Cyclin Dependent Kinase 6	CCTGCAGGGAAAGAAAAGTGC	CCTCCTCTCCCTCCTCGAA
<b>CDK7</b>	Cyclin Dependent Kinase 7	GTGGCCGGACATGTGTAGTC	GCCGTAATTCGAGCACATGG
<b>CDK9</b>	Cyclin Dependent Kinase 9	ATGGAAAACGAGAAGGAGGGG	TAGGGGGAAGCTTTGGTTTCG
<b>CDKN1 A</b>	Cyclin Dependent Kinase Inhibitor 1A	TCTTGTACCCTTGTGCCTCG	CGGCGTTTGGAGTGGTAGAA
<b>CDKN1 B</b>	Cyclin Dependent Kinase Inhibitor 1B	GGCTAACTCTGAGGACACGC	TGAGTAGAAGAATCGTCGGTTG C
<b>CDKN2 C</b>	Cyclin Dependent Kinase Inhibitor 2C	AGAAACTGTCACTGGGAGCG	AGGCTCGGCCATTCTTTAGG
<b>CDKN2 D</b>	Cyclin Dependent Kinase Inhibitor 2D	GGCAGTTCAAGAGGGTCACA	GTCCCTGCGATGGAGATCAG
<b>CHEK1</b>	Checkpoint Kinase 1	GGTCACAGGAGAGAAGGCAAT A	GGAAGAATCTCTGAGCATCTGG
<b>CHEK2</b>	Checkpoint Kinase 2	AGTGGATCCAAAGGCACGTT	CCTGGGGTAGAGCTGTGGAT
<b>CITED2</b>	Cbp/P300- Interacting Transactivator With Glu/Asp Rich Carboxy- Terminal Domain 2	GCGAGCACATACACTACGGC	CCATGAACTGGGAGTTGTAAAC C
<b>CKIT</b>	KIT proto- oncogene	GCATTCAAGCACAATGGCAC	CCAATCAGCAAAGGAGTGAA
<b>DOT1L</b>	Disruptor of Telomeric Silencing 1- Like	CAGTGAGAAGGGCCTGAGAG	TGGAGTTGAGGTTGAGGGGA
<b>ENOX2</b>	Ecto-NOX disulfide-thiol exchanger 2	CACTGGCACTACCAAAGTGA	GAGCTGGAGGGAACCTGATTT

<b><i>GUSB</i></b>	Glucuronidase beta	GAGCAAGACAGTGGGCTGG	CCATTCGCCACGACTTTGTT
<b><i>HIF1A</i></b>	Hypoxia Inducible Factor 1 Subunit Alpha	TACTCATCCATGTGACCATGAGG	TAGTTCTTCCTCGGCTAGTTAGG
<b><i>HOXA9</i></b>	Homeobox A9	CCCCATCGATCCCAATAACCC	TCCCTGGTGAGGTACATGTTG
<b><i>IRF1</i></b>	Interferon Regulatory Factor 1	ACCTCTGCCTTCTTCCCTCT	CATCCGAGTGATGGGCATGT
<b><i>JUN</i></b>	Jun proto-oncogene, AP-1 transcription factor subunit	GGGGTTGACTGGTAGCAGAT	CTGTGTCTGTCTGTCTGCCT
<b><i>MCL1</i></b>	Myeloid Cell Leukaemia 1	GCCTTCCAAGGATGGGTTTG	TATGCCAAACCAGCTCCTACTC
<b><i>MEIS1</i></b>	Meis Homeobox 1	ATGGCGCAAAGGTACGACG	TACTGATGCGAGTGCAGAGG
<b><i>MYC</i></b>	MYC proto-oncogene, bHLH transcription factor	GACTCTGAGGAGGAACAAGA	TCGTCCGAGTAGAAATACGG
<b><i>TP53</i></b>	Tumour Protein p53	TGTGACTTGCACGTACTCCC	TCCGTCATGTGCTGTGACTG
<b><i>SOX9</i></b>	SRY-box transcription factor 9	ATCTCCCCCAACGCCATCTT	CTGGGATTGCCCCGAGTG
<b><i>TBP</i></b>	TATA-box binding protein	ATCTTTGCAGTGACCCAGCAT	CTTGCGCTGGAACTCGTCT
<b><i>TP73</i></b>	Tumour Protein p53	ACTTTGAGATCCTGATGAAGC	GAGGACCGGCCCGTAGGA
<b><i>TYW1</i></b>	TRNA-YW Synthesizing Protein 1 Homolog	CTCCTGATAGCACACAGAAAGTTTA	TGCGCTGAACGTTTTTGATCC
<b><i>VEGF</i></b>	Vascular Endothelial Growth Factor	AGAAGGAGGAGGGCAGAATCA	AGGGTACTCCTGGAAGATGTCC